

tures in the measured optical spectrum with the electronic transitions between energy bands but also for other purposes, such as a calculation of the phonon frequencies.

We are grateful to Dr. Z. Kam for his help with the Gilat-Raubenheimer program and to Professor W. Kohn for stimulating discussions.

*Work supported in part by the National Science Foundation under Grant No. GH-38345.

†Work supported in part by the Deutsche Forschungsgemeinschaft and by the Max-Planck Institut für Festkörperforschung, Stuttgart, Germany.

¹S. L. Adler, Phys. Rev. 126, 413 (1962); N. Wiser, Phys. Rev. 129, 62 (1963).

²T. K. Bergstresser and G. W. Rubloff, Phys. Rev. Lett. 30, 794 (1973).

³W. Hanke, Phys. Rev. B 8, 4585, 4591 (1973), and in *Proceedings of the International Conference on Phonons, Rennes, France, 1971*, edited by M. A. Nusimovici (Flammarion, Paris, 1971), p. 294, and in *Proceedings of the International Conference on Inelastic*

Scattering of Neutrons, Grenoble, France, 1972 (International Atomic Energy Agency, Vienna, 1972), p. 3; L. J. Sham, Phys. Rev. B 6, 3584 (1972), and in *Lattice Dynamics*, edited by A. A. Maradudin and G. K. Horton (North-Holland, Amsterdam, to be published).

⁴J. A. Van Vechten and R. M. Martin, Phys. Rev. Lett. 28, 446 (1972).

⁵L. J. Sham and J. M. Ziman, Solid State Phys. 15, 282 (1963).

⁶V. Ambegaokar and W. Kohn, Phys. Rev. 117, 423 (1960).

⁷S. K. Sinha, R. P. Gupta, and D. L. Price, Phys. Rev. Lett. 26, 1324 (1971), and Phys. Rev. B 9, 2564, 2573 (1974).

⁸G. G. Hall, Phil. Mag. 43, 338 (1952).

⁹L. Pauling, J. Amer. Chem. Soc. 53, 1367 (1931).

¹⁰G. S. Painter, D. E. Ellis, and A. R. Lubinsky, Phys. Rev. B 4, 3610 (1971).

¹¹G. Gilat and L. J. Raubenheimer, Phys. Rev. 144, 390 (1966).

¹²R. A. Roberts and W. C. Walker, Phys. Rev. 161, 730 (1967).

¹³A. R. Lubinsky, D. E. Ellis, and G. S. Painter, Phys. Rev. B 6, 3950 (1972).

¹⁴R. N. Euwema, D. L. Wilhite, and G. T. Surratt, Phys. Rev. B 7, 818 (1973).

Direct Transform-Deconvolution Method for Surface-Structure Determination

David L. Adams and Uzi Landman

Chemistry Research Laboratory, Xerox Corporation, Webster, New York 14580

(Received 6 March 1974)

We describe direct method for surface-structure determination from low-energy electron-diffraction (LEED) intensities. Fourier transforms of LEED intensities are shown to contain convolution products of functions of the interatomic vectors with data truncation and potential windows. A deconvolution method and substrate-subtraction procedure is described, yielding an accurate structural determination of clean surfaces and overlayer systems. Applicability of the method to experimental data is demonstrated by using LEED intensities from Al(100).

Since the discovery¹ of low-energy electron diffraction (LEED), the extraction of surface structures has been the subject of intensive efforts, mainly via an *indirect approach*,² which is intrinsically dependent on model assumptions and proceeds by comparisons of microscopic model calculations with experimental intensities. However, a full variation over the geometrical and electronic parameters is not carried out because of the prohibitive expense in computation time and storage.

In this paper we present the principles of a rapid, *direct method* of surface-structure determination³ and demonstrate its applicability to the analysis of experimental data.⁴

In the diffraction of low-energy electrons from solids, momentum is conserved in the plane parallel to the surface, giving rise to diffracted beams characterized by discrete (hk) Miller indices of the two-dimensional net. Electron propagation in the direction normal to the surface is strongly attenuated¹ and is, therefore, characterized by the continuous variable S , where $2\pi S$ is the normal momentum transfer and $S > 0$ as a result of the half-space nature of LEED measurements and the inner potential

of the solid. Consequently, the complex Fourier transform of the intensities may be written as

$$P(x, y, z) = \sum_{h, k = -\infty}^{\infty} \int_{-\infty}^{\infty} dS I_{hk}(S) \omega_B(S; S_1, S_2) \exp[2\pi i(hx + ky)] \exp(2\pi iSz), \quad (1)$$

where $I_{hk}(S)$ is the intensity of the (hk) beam and $\omega_B(S; S_1, S_2)$ is a "box-car" truncation function (unit magnitude for $S_1 < S < S_2$ and zero otherwise).

The transformation given in Eq. (1) defines a *three-dimensional vector space*.⁵ Structure determination, however, can be carried out by using reduced forms of the three-dimensional transform. The analysis proceeds by the determination of interlayer spacings from *one-dimensional projections* of the transform, the result of which are utilized in the determination of interlayer registries via *two-dimensional transform sections* as we have previously demonstrated.³ The one-dimensional line projection $P(z)$ is defined by

$$P(z) = \int_{-\infty}^{\infty} dS I_{00}(S) \omega_B(S; S_1, S_2) \exp(2\pi iSz), \quad (2)$$

where I_{00} is the intensity of the specular beam. As shown below analytically for the case of kinematic scattering, and through analysis of experimental data exhibiting pronounced multiple-scattering features, $P(z)$ contains the projections of interatomic vectors on the surface normal. As we have indicated previously, the problems of deconvolution, discussed below, are most acute in the analysis of line projections.

The fundamental problem involved in the use of the LEED transform consists of the extraction of geometrical information from its convolution with the effects of data truncation, scattering potentials, and temperature. We emphasize that failure to perform a proper deconvolution results in most cases in ambiguous structural assignments and inadequate spatial resolution.^{6,7}

The scattering amplitude and hence the diffracted intensity can be expressed as a series expansion in the order of scattering events. Hence, the transform of the intensity consists of a linear combination of transforms of n th order scattering processes ($n=1, 2, 3, \dots$) which can be expressed in turn as convolution products of geometrical and electronic and vibrational factors. However, we anticipate that the first-order convolution product will produce the dominant features in the transform. Multiple-scattering contributions to the diffracted intensities are generally aperiodic with momentum transfer, and are effectively attenuated by Fourier transformations.

The above conclusions are supported by results of numerical studies⁸ using intensities calculated from a full multiple-scattering theory, and by the application of the deconvolution method to the analysis of experimental data exhibiting pronounced multiple-scattering features, as described below and in detail elsewhere.⁴ Accordingly, we now demonstrate the principles of the transform-deconvolution method, using kinematical theory with realistic scattering potentials and inclusion of temperature effects.

The kinematical expression for the intensity of specularly diffracted electrons from a lattice composed of a uniform substrate with layer spacing d_s and an overlayer at a distance d_o from the surface plane is given by

$$I(S) = |f_o(S)|^2 + 2|f_s(S)|^2 \alpha_o^2 (1 - \alpha_s^2)^{-1} \sum_{\nu=0}^{\infty} (\alpha_s^\nu \cos \varphi_\nu - 1) + 2\alpha_o \sum_{\nu=0}^{\infty} \alpha_s^\nu [f_{os}(S) \cos(\varphi_\nu + \beta) + f_{os}^\dagger(S) \sin(\varphi_\nu + \beta)], \quad (3)$$

where $\alpha_s = \exp(-\mu'_s d_s)$, $\alpha_o = \exp(-\mu'_o d_o)$, and $\mu' = \mu / \cos \theta$ with μ the attenuation coefficient¹ and θ the angle of incidence. The phase angles are defined as $\varphi_\nu = 2\pi S \nu d_s$ and $\beta = 2\pi S d_o$. $f_{s,o}(S)$ are the effective atomic scattering factors, renormalized to incorporate atomic vibrations⁹ by multiplication by the associated Debye-Waller factors, of the substrate (s) and overlayer (o) which can be expressed in a partial-wave expansion with scattering-potential phase shifts¹⁰ $\delta_{s,l}(S)$ and $\delta_{o,l}$ for the substrate and overlayer, respectively. The function $f_{os}(S)$ is defined as $f_{os}(S) = f_o(S) f_s^\dagger(S)$. The transform [Eq (2)] of the above intensity expression is given by

$$P_o(z) = F_o(z) * \delta(z) + F_s(z) * \alpha_o^2 (1 - \alpha_s^2)^{-1} \sum_{\nu=-\infty}^{\infty} \alpha_s^{|\nu|} |\delta(z + d_s) + \alpha_o \sum_{\nu=0}^{\infty} \alpha_s^\nu [F_{os}(z) * \delta(z - d_o - \nu d_s) + F_{so}(z) * \delta(z + d_o + \nu d_s)], \quad (4)$$

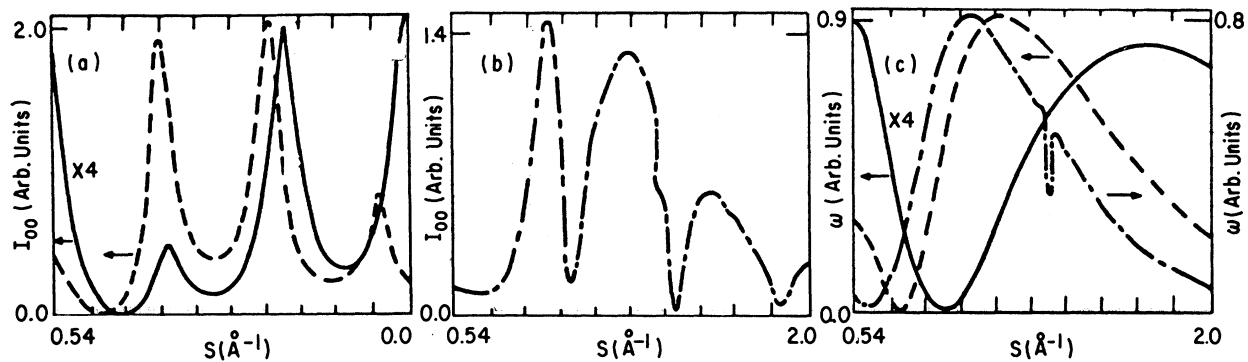


FIG. 1. Calculated intensities (a) for Al(100) (solid and dashed curves, $\theta = 25^\circ$ and 8° , respectively) and (b) for Na overlayer on Al with $d_o = 2.2 \text{ \AA}$ (dash-dotted curve, $\theta = 8^\circ$) using four phase shifts (Ref. 12). (c) Substrate ω_s (solid and dashed curves for $\theta = 25^\circ$ and 8° , respectively) and overlayer (dash-dotted curve for $\theta = 8^\circ$) potential windows, corresponding to the above intensities.

where the asterisk denotes convolution and F_o , F_s , $F_{o,s}$, and $F_{s,o}$ are the transforms of $|f_o|^2$, $|f_s|^2$, $f_o f_s^\dagger$, and $f_o^\dagger f_s$, respectively, convoluted with the transform of the "box-car" window ω_B defined in Eq. (1). In the following we refer to the functions $\omega_{o,s} = |f_{o,s}|^2 \omega_B(S; S_1, S_2)$ as the potential envelopes (windows) for the overlayer (o) and substrate (s), respectively.

The second term in the above equation with the substitution $\alpha_o = 1$ is the transform $P_s(z)$ of the clean-substrate intensity. It consists of peaks at $z = \nu d_s$ ($-\infty < \nu < \infty$), weighted by the damping factors $(1 - \alpha_s^2)^{-1}$, convoluted with the transform of the truncated atomic scattering potential. Thus, a transformation of the intensities diffracted from a clear surface followed by a deconvolution of the complex transform $F_s(z)$ yields a "delta-function transform." Because of the idempotency of the window matrix, conventional matrix-inversion algorithms cannot be applied in the deconvolution. A solution to this crucial problem has been formulated by modifying a relaxation method described by Southwell.^{11,8}

The deconvolution is demonstrated first for the clean substrate. Figure 1(a) contains calculated kinematical intensities for the (00) beam from Al(100), for two incident angles, and $T = 0^\circ\text{K}$; Figure 1(c) contains the associated potential envelopes. The Fourier transforms of the intensity records are given in Figs. 2(a) and 2(b), from which it is evident that peak broadening and extra peaks due to the truncated potential envelopes preclude *direct* structural interpretation. The computer deconvolutions^{4,8} of the truncated potential windows from the transforms for $\theta = 8^\circ$ and 25° are identical. The unique result is shown in Fig. 2(c).

Interpretation of the transform [Eq. (4)] of the intensity diffracted from an overlayer system is complicated by the convolution of maxima which are structural in origin with functions associated with the differences in scattering potential of the substrate and overlayer atoms. An accurate determination of the overlayer geometry is achieved by the *substrate subtraction* method defined as

$$P_{\text{RES}}(z) = P_o(z) - gP_s(z) - \delta(z) * F_o(z), \quad (5)$$

where P_o and P_s are the overlayer and substrate transforms, respectively. For $g = \alpha_o^2$,

$$P_{\text{RES}}(z) = \alpha_o \sum_{\nu=0}^{\infty} \alpha_s^\nu [F_{o,s}(z) * \delta(z - d_o - d_s) + F_{s,o}(z) * \delta(z + d_o + \nu d_s)]. \quad (6)$$

Optimum substrate subtraction is achieved by a variation of g in Eq. (5) to minimize

$$\sum_{\nu=0}^{\infty} P_{\text{RES}}(\nu d_s).$$

Determination of the overlayer spacing is demonstrated for the case of a Na overlayer on Al(100). A calculated (00) intensity for an arbitrarily

chosen overlayer spacing $d_o = 2.2 \text{ \AA}$ and $\theta = 8^\circ$ using a four-phase-shift expansion in the description of the substrate and overlayer scattering potentials is shown in Fig. 1(b) along with the overlayer potential envelope $|f_o|^2$ in Fig. 1(c). It is again evident that structure determination cannot be made solely on the basis of the correspond-

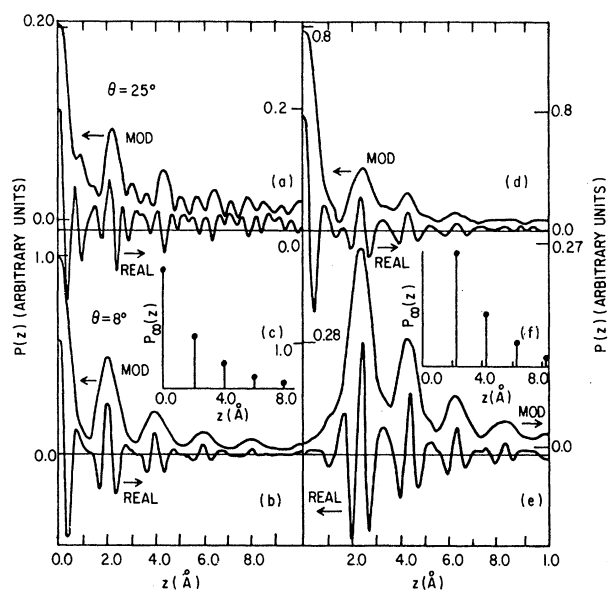


FIG. 2. (a), (b) Modulus and real part of the $P(z)$ transforms derived from the intensities shown in Fig. 1(a). (c) Computer deconvolution (P_∞) (Ref. 8) obtained by deconvoluting the transform of the windows in Fig. 1(a) from the transforms shown in (a) and (b). (d) $P(z)$ transform for the overlayer intensity [Fig. 1(b)]. Note the absence of peaks at substrate spacings. (e) Substrate-subtraction residuals [Eq. (5)], obtained from the transforms shown in (b) and (d). (f) Computer deconvolution (P_∞) (Ref. 8) of the residual, exhibiting highly resolved peaks corresponding to the substrate-overlayer vectors.

ing transforms which are shown in Fig. 2(d). The *residual transform*, $P_{\text{RES}}(z)$, derived from the transforms shown in Figs. 2(b) and 2(d) is shown in Fig. 2(e). Deconvolution of the residual transform yields the overlayer-substrate interlayer vectors as shown in Fig. 2(f).

We now illustrate the applicability of the transform-deconvolution method to experimental data. In Fig. 3(a) we present (00) intensity profiles measured⁴ at room temperature from Al(100) for $\varphi = 0^\circ$ and $\theta = 8^\circ$ and 16° . The real parts of their transforms are shown in Fig. 3(b). We draw attention to the pronounced multiple-scattering features in the intensity profiles, and to the vibrations in both the intensity profiles and their transforms with angle of incidence. In constructing appropriate potential envelope windows for deconvolution of transforms such as are shown in Fig. 3(b) we have used eight phase shifts calculated from Snow's potential.¹³

The deconvolution results shown in Figs. 3(c)

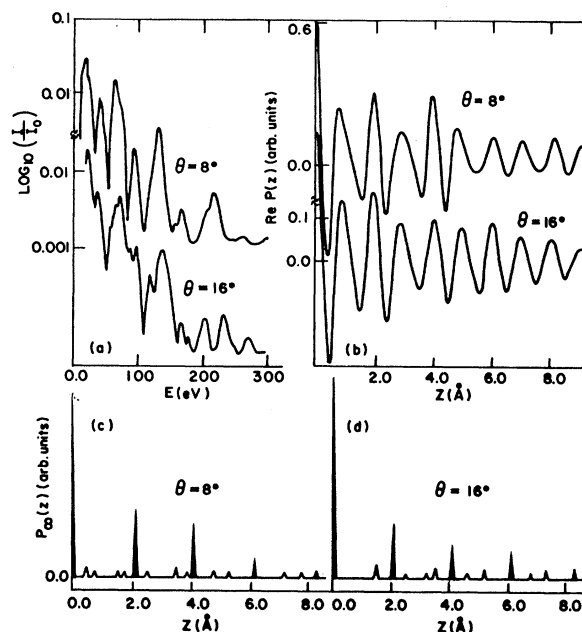


FIG. 3. (a) (00) intensities from Al(100) measured at $T = 295^\circ\text{K}$ for $\varphi = 0$, $\theta = 8^\circ$ and 16° . (b) Real part of the $P(z)$ transforms of the intensities shown in (a). (c), (d) Computer deconvolutions (P_∞) of the transforms shown in (b) ($\theta = 8^\circ$ and 16° , respectively). The base width of the peaks is 0.05 \AA . Structural peaks forming a consistent vector set have been filled. The use of eight phase shifts (Ref. 13) in the potential window resulted in a suppression of "noise" level (open peaks).

and 3(d) for $\theta = 8^\circ$ and 16° , respectively, were obtained by using optimized values of the inner potential and effective Debye temperature of 14 eV and 300°K , respectively. In comparing these results with those obtained from calculated kinematic intensities shown in Fig. 2, it can be seen that in addition to the prominent structural peaks in Figs. 3(c) and 3(d) there is a low level of noise. (Similar noise peaks of *negative* amplitude have been suppressed in the figures since obviously they convey no structural information. *Convoluting* the total deconvolution results with the corresponding potential windows used reproduces the observed transforms to better than 1%.)

In the above results, and in results for other angles of incidence,⁴ prominent peaks occur only at $2.05N \text{ \AA}$ ($N = 0, 1, 2$, etc.) and form the only consistent periodic vector set. The unique value of the interlayer spacing determined from different intensity profiles, despite their strong variation with angle of incidence, demonstrates the consistency of the method and illustrates its applicability. We note that the determined value 2.05 \AA is

in agreement with the bulk interlayer spacing of 2.025 Å to within our estimated accuracy of ± 0.05 Å. In addition it compares with the conclusions of extensive multiple-scattering calculations.¹⁴

Further details of our method and applications to experimental data are given in forthcoming publications.^{4,8}

We are indebted to Dr. E. P. Goldberg and Dr. M. L. Hair for their encouragement and interest, and to Mr. J. C. Hamilton for helpful discussions.

¹C. J. Davisson and L. H. Germer, *Phys. Rev.* **30**, 705 (1927).

²*Phys. Today* **27**, No. 3, 17 (1974).

³U. Landman and D. L. Adams, *J. Vac. Sci. Technol.* **11**, 195 (1974).

⁴D. L. Adams, U. Landman, and J. C. Hamilton, to

be published.

⁵M. J. Burger, *Vector Space* (Wiley, New York, 1954).

⁶J. C. Buchholz, M. G. Lagally, and M. B. Webb, *Surface Sci.* **41**, 248 (1974).

⁷T. A. Clarke, R. Mason, and M. Tescari, *Surface Sci.* **30**, 553 (1972), and **40**, 1 (1973), and *Proc. Roy. Soc., Ser. A* **331**, 321 (1972).

⁸U. Landman and D. L. Adams, to be published.

⁹G. E. Laramore, *Phys. Rev. B* **6**, 1097 (1972).

¹⁰L. I. Schiff, *Quantum Mechanics* (McGraw-Hill, New York, 1955).

¹¹R. V. Southwell, *Relaxation Methods in Theoretical Physics* (Oxford Univ. Press, Oxford, England, 1946).

¹²C. B. Duke, N. O. Lipari, and U. Landman, *Phys. Rev. B* **8**, 2454 (1973).

¹³The authors are indebted to Dr. J. E. Demuth and Dr. P. Marcus for supplying us with the phase shifts used in this calculation.

¹⁴D. W. Jepsen, P. M. Marcus, and F. Jona, *Phys. Rev. B* **5**, 3933 (1972).

Backward Scattering in the One-Dimensional Electron Gas*

A. Luther†

Lyman Laboratory, Harvard University, Cambridge, Massachusetts 02138

and

V. J. Emery

Brookhaven National Laboratory, Upton, New York 11973

(Received 16 July 1974)

An exact solution to the one-dimensional electron gas with a particular attractive-interaction strength for scattering across the Fermi "surface" is given. It is shown that conductivity enhancement occurs for physically interesting values of the coupling constants. Scaling arguments are advanced to demonstrate that this solution applies generally for attractive backward scattering. In addition, the spinless problem is solved exactly for arbitrary couplings.

Progress towards an understanding of the equilibrium and transport properties of quasi-one-dimensional conductors has been hampered by a lack of knowledge about the underlying interacting electron system. Although the Tomonaga and Luttinger models¹ have provided some insight, their generality can be questioned as a result of their neglect of interactions near twice the Fermi momentum, $2k_F$, which are responsible for backward scattering. This note reports an exact solution to the more general problem with an attractive interaction at $2k_F$, and uses it to construct a qualitative picture for the general interacting one-dimensional system.

Several properties of the exact solution are particularly significant. It requires an attractive interaction at $2k_F$ of a specific strength but the small-momentum interaction can be arbitrary, a situation of sufficient generality to be of interest for experiments on the quasi-one-dimensional systems. Depending upon the sign and magnitude of the small-momentum part, a large conductivity enhancement can occur as the temperature tends to zero, in contrast to a recent approximate treatment.² We compute the temperature dependence of the conductivity as well as other physically important response functions which describe the low-temperature pairing, charge and spin